Numerical Analysis of Powder Compaction to Obtain High Relative Density in '601AB' Aluminum Powder

Ranjit Kumar Verma[1], Mahesh N. S. [2], Anwar M. I.[3]

1- M.Sc. [Engg.] Student, 2-Professor and Head,
Department of Mechanical and Manufacturing Engineering,
M. S. Ramaiah School of Advanced Studies, Bangalore 560 058

Abstract

Many advantages are inherent to successful powder metallurgy (P/M) process especially in high volume manufacturing. The process consists of a compaction stage (produces low strength green part) and a sintering stage (bonds particles together thereby increases parts strength). The strength/density distribution of the compacted product is crucial to overall success. The finite element analysis (FEA) has become an effective way to numerically simulate strength/density distribution in a P/M compact.

The objective of the study was to simulate compaction process to achieve uniform and high bulk density green parts. A material model (Cam-Clay) which can capture the particle re-arrangement under compaction process has been adopted. An axi-symmetric analysis has been followed on 601AB aluminium alloy powder with initial apparent density as 40%.

A finite element model with upper and lower punch displacement control was formulated and solved in ABAQUS. The study revealed that, 55 to 56% (in this case 14mm) of the punch displacements can result in 100% relative density at upper and lower corners. It was observed that maintaining friction coefficient 0.15 to 0.2 would produce better density distribution in the powder compact. H/D ratio recommended for obtaining higher and uniform relative density for 56% compaction is 2-3. Higher H/D will result in large variation in relative density distribution whereas lower H/D result in less than 100% density in any portion of the compact.

Key Words: Powder Compaction, 601AB Aluminum Powder.

1. INTRODUCTION

Knowledge of the behavior of powder material undergoing cold compaction is necessary for predicting the final shape and density distribution within the parts, and for preventing failures that can occur during subsequent sintering. The powder compaction process transforms loose powder into a compacted sample, with an increase in density.

The compaction process consists of a die filling stage where controlled amount of the powder is fed into the die cavity and top and bottom punches moves to press the powder. The P/M process can produce net or near-net shape parts with complicated geometries that are difficult to produce by conventional machining approaches. Often, one powder compaction process replaces two or more conventional machining processes. This advantage reduces set-up time, inventory and manufacturing costs

Atomization is the most widely used process to produce aluminum powder [1]. Aluminum is melted with addition of elemental alloy (copper, magnesium and silicon) and then sprayed through a nozzle to form a stream of very fine particles that are rapidly cooled by an expanding gas. The size of the particles formed depends on the temperature of the metal, metal flow rate through the orifice, nozzle size and jet characteristics.

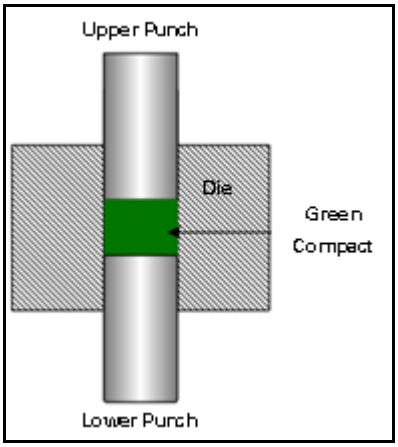

Fig. 1 Schematic of a die compaction process

It has been reported that small particles generate a lot of inter-particle friction due to higher surface areas [3]. This restricts the powders flow rate. Also, apparent density of small powders is higher than that of big powders of the same material. During compaction small metallic particles originates problems such as longer time to fill the matrix, damages due to wear in die and tooling elements which directly effects productivity [4]. Hence, the particles of most powders used for compacting have irregular equiaxed shape, with flow rates between those of spherical (high flow rates) and flaky (low flow rates) powders [1].

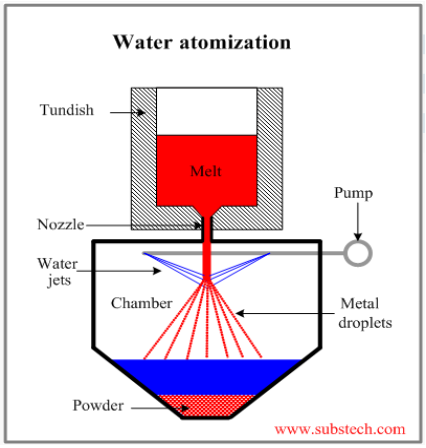

Fig. 2 Schematic of water atomization process [2]

2. FINITE ELEMENT MODELS

Finite element methods (FEM) can be used to predict various characteristics of the process such as green density distributions, powder flow, stresses in powder and compact, effect of H/D ratio and frictional co-efficient and stresses developed in the die parts, etc. Hence FEA simulation must help to reduce the on-the-floor trial and error type of process development by varying its process parameter with ease.

Based on available literatures; a popular approach adopted by many researchers in their work was the continuum modeling approach (Weber and Brown, 1992, Mosbah and Bouvard, 1996, Trasorras,et al, 1992, Bandstra, et al, 1990 and many more) with the proper selection of a material model (Cam-Clay) to describe the complex nature of the process from lose aggregation of particles to a continuous skeleton structure.

2.1 Cam-Clay model

Many authors have used the Cam-Clay model in their attempt at modeling powder compaction. This model was developed by Roscoe and Schofield et al., 1968 and Parry, 1972, at Cambridge University. It contains: a yield surface, and a critical state surface that is the locus of effective stress.

2.1.1 Yield Surface

The equation of the yield surface used in ABAQUS [5] is.

$$f(p,q)=\frac{1}{\beta^2}\left(\frac{p}{a}-1\right)^2+\left(\frac{q}{Ma}\right)^2-1=0$$

And the equation of the critical state line is

q=Mp

Where,
P is the Mean stress, q is the equivalent Mises stress,
M is a constant that defines the slope of the critical state line,
a is a hardening parameter that defines the size of the yield, surface and β are user-specified material parameters

p and q are defined as

$$p=-\frac{1}{3}(\sigma_1+\sigma_2+\sigma_3)$$

$$q=\sqrt{\frac{3}{2}S:S}$$

Where S is the deviatoric stress (S=σ + pI), σ is the stress tensor.

Note: Collection of all the yield stress points in the p-q space forms the yield surface.

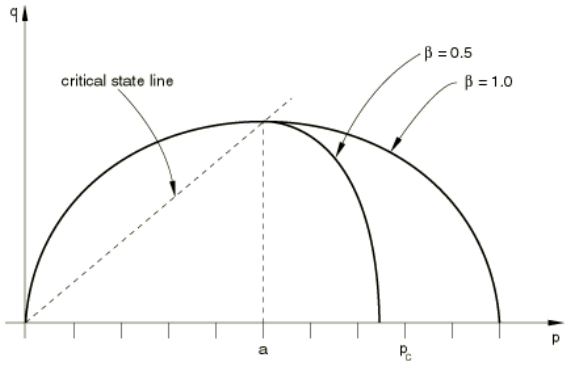

Fig. 3 Typical yield surfaces [5]

2.1.2 Hardening Behavior

The hardening law controls the size of the yield surface in the effective stress (p-q) space. The size of the yield surface at any time is determined in terms of the hardening parameter, a. It depends on the volumetric plastic strain component. When the volumetric plastic strain is compressive (i.e. when the soil is compacted), the yield surface grows in size. An inelastic increase in the volume causes the yield surface to shrink. The hardening law can be written in below exponential form as mentioned in the ABAQUS [5].

$$a=a_0\exp\left[(1+e_0)\frac{1-J^{pl}}{\lambda-kJ^{pl}}\right]$$

$$a_0=\frac{1}{2}\exp\left(\frac{e_1-e_0-\kappa\ln p_0}{\lambda-\kappa}\right)$$

Where,
a_0 is the initial value of the hardening parameter
J^{pl} the inelastic volume change (the ratio of current volume to initial volume)
k is the logarithmic bulk modulus of the material (defined for the porous elastic material)
λ is the logarithmic hardening constant and
e_0 is the user-defined initial void ratio
p_0 is the initial value of the equivalent hydrostatic pressure stress
The initial size of yield surface is expressed by specifying the initial value of the hardening parameter, a_0. This parameter is dependent only on the initial conditions and does not vary with temperature or any other field variables change during the analysis. It can be

expressed in terms of the intercept of the virgin consolidation line with the void ratio axis, e_1, in the plot of void ratio versus logarithm of the effective pressure stress, *ln*p

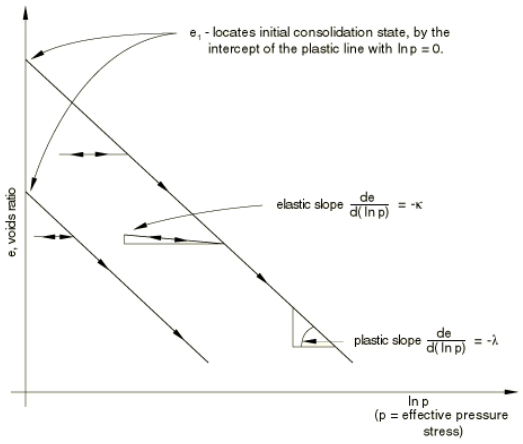

Fig. 4 Compression behaviour-clay model [5]

2.1.3 Calibration

At least two experiments are required to calibrate the simplest version of the Cam-Clay model: a hydrostatic compression test (an oedometer test is also acceptable) and a triaxial compression test (more than one triaxial test is useful for a more accurate calibration) [5].

3. GEOMETRICAL MODEL

The sample used for the compaction analysis was assumed as an axi-symmetric cylinder with initial fill height of 50 mm and 30 mm diameter. This model takes advantage of symmetry about the midplane, as well as the axisymmetry of the configuration. Due to symmetry, only half of the cross section was considered and finely meshed near the die-compact interaction region rather close to axis region.

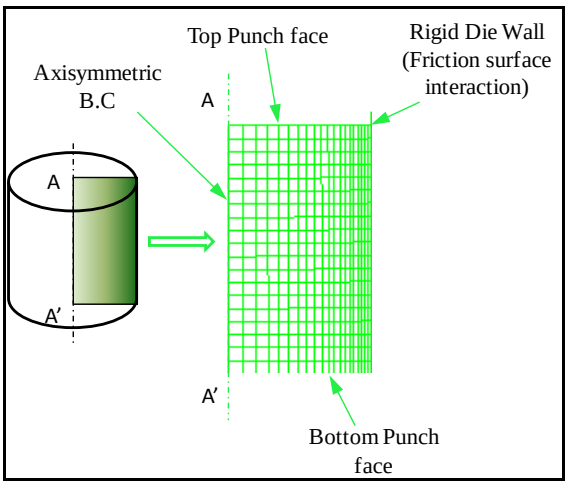

Fig. 5. Axi-symmetric geometry and Mesh

4. GRID INDEPENDENCE STUDY

Grid size plays an important role in both convergence and accuracy of the solution. A course mesh is used to quickly examine the solver settings and boundary conditions. The use of high-density mesh improves the accuracy of simulation, but is computationally expensive. Hence grid independence studies are performed to obtain an optimized mesh size. For the current problem, initially a coarse mesh with 660 elements was used to do the compaction analysis. The element density was subsequently increased to 1300, 2772, 6000 and 15000. The simulations were performed for 56% compaction of initial height. Figure 6 shows the grid independence study graph for the powder compaction where punches was emulated from both the sides. The error between the simulations using higher mesh densities was less than 1% and hence all further analyses were done using grid size of not less than 6000 elements.

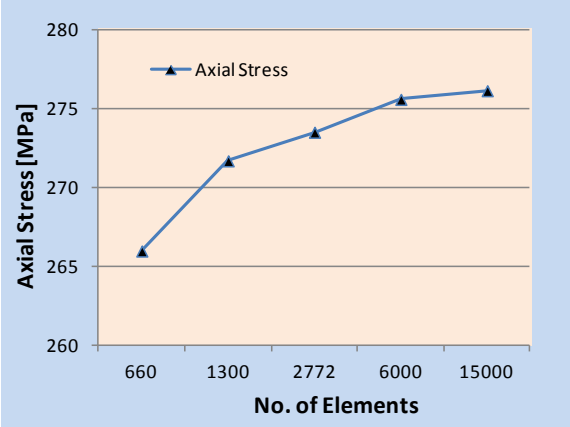

Fig. 6. Grid independence study

5. SOLUTION METHODOLOGY

- Effect of displacement on compact was studied in order to achieve maximum and uniformly distributed green parts.
- Effect of die wall friction was studied in order to find the range of coulomb friction to be maintained to achieve better density distributed green pats.
- Effect of initial fill height was studied in order to find a better height to diameter (H/D) ratio for uniform and higher relative density.

Note: all the simulations were carried out by considering secondary deflection effect (i.e NLGEOM=ON in ABAQUS).

6. RESULTS AND DISCUSSION

6.1 Effect of displacement on green density

To fix the displacement (final height) of the punch during the compaction process a trials on the 50mm initial fill height and 30mm diameter with 40% apparent density model were conducted and the variation in relative density, as displacement advances from the external surfaces (Top and Bottom) is presented in figure 7.

It is seen from figure 7 that, during initial stage of compaction, there is no significant change in density. However a significant change in slope is observed as compaction progresses.

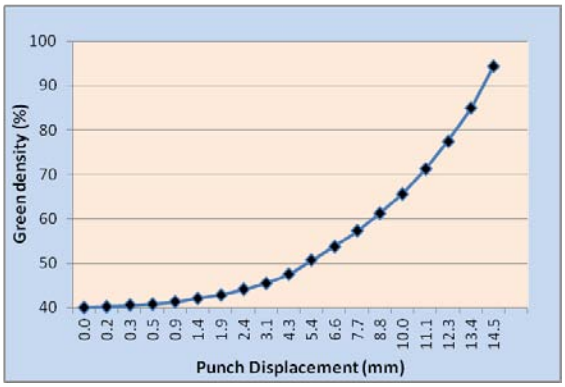

Fig. 7 Green (relative) density variations

Contour plots for 14mm compaction is presented in the figure 8. A slight change in density variation was observed as displacement advances.

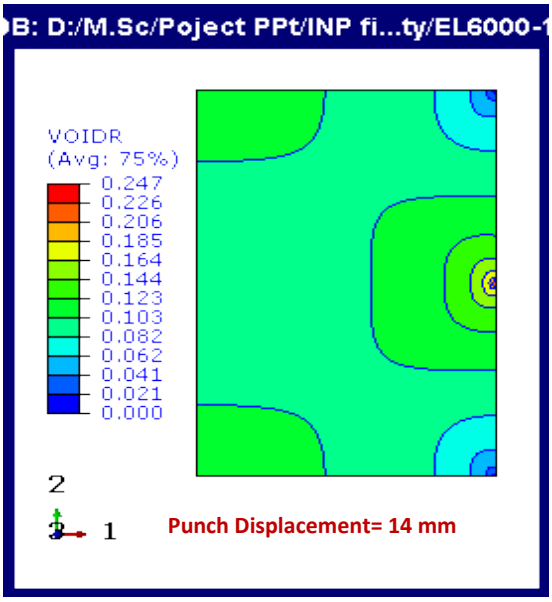

Fig. 8 VOIDR pattern for 14mm compaction

The figure 8 shows that, 100% relative density could be achieved on the top and bottom corner surfaces when the final height of component reaches to 22 mm (14 mm displacement on both the punches).

The density variation along the die wall for various stages of compaction is plotted in figure 9. There is a change in slope noticed in the figure as punch advances from 12 to 15mm.

Figure 9 shows that, when punch displacement increases relative density of the compact increases. For punch displacement 14 mm the maximum density observed in the top and bottom corner is 100% and density decreases uniformly till 86% in the vicinity of center. Large change in slope observed near the punches areas are due to applied compaction loads causing radial forces towards the die walls.

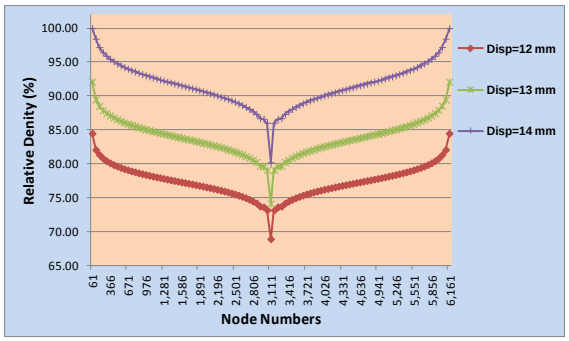

Fig. 9 Density variations along the die wall

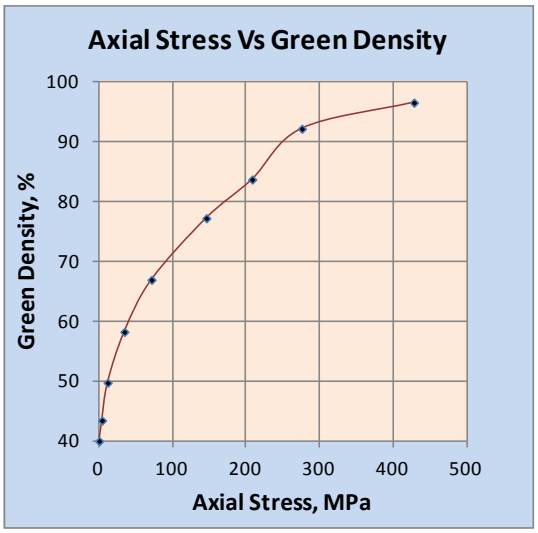

Fig. 10 Axial stress Vs Green density variations

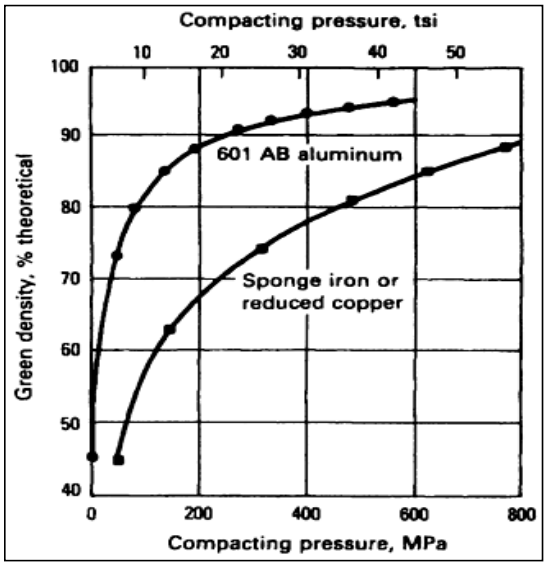

Fig. 11 Experimental data [1]

For validation purpose the axial stress data obtained from simulation for 601AB aluminum alloy are plotted (Axial stress Vs Green density) and compared with the die pressing test result presented in the ASM Handbook [1], (figure 10 and 11). It is observed that the axial stress variation obtained from Cam-Clay is similar to the test result presented in the ASM Handbook [1]. Finite element analysis with upper and lower punch displacement control revealed that the maximum compression is ~55-56% of the original height (in this case 50*0.56=28 mm) for 601AB alloy.

6.2 Effect of die wall friction (μ) on density

Presence of friction between powder particles and die wall reduces the flow ability of the compact in the die, hence affects the characteristics of the part. Therefore for accurate prediction of the effect of friction on the density distribution is important. The study suggests that friction coefficient changes with pressure and density, though a constant friction coefficient is considered throughout the simulation to study the effect of varying value of 'μ'. The range of values used for the friction coefficient covers those reported in literature for metallic powders (0.08-0.4). For the mesh model, contact interaction was defined between the powder and the die wall using a friction surface interaction in ABAQUS.

Simulations were carried out for μ=0.08, 0.1, 0.15, 0.2, 0.3 and 0.4 to study the effect of varying values of coefficient of friction. The maximum and minimum density, axial stresses in the part was studied with respect to the friction coefficient. Void Ratio (VOIDR) distributions for the μ=0.15 are shown in figures 12. Maximum density (minimum VOIDR) is observed at the punch corners and these magnitudes diminishe away from the punch as pressure tapers off gradually towards center of the components. Maximum density achieved in this case is 100% at the upper and lower edge, whereas minimum density achieved is 81% at the center of the compact.

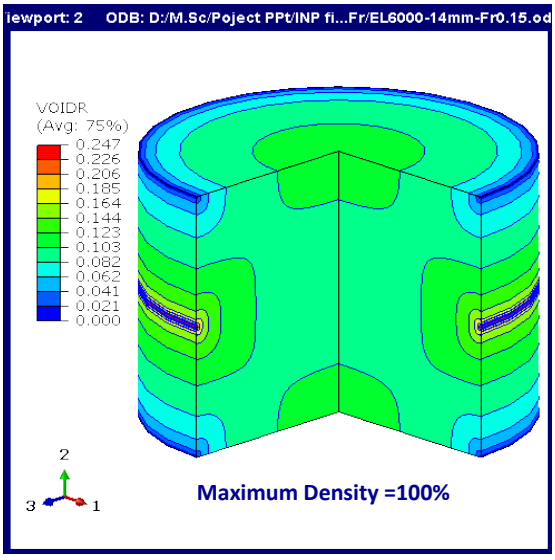

Fig. 12 VOIDR distributions for 'μ=0.15'

Figure 13 illustrate graph plots variation in density (difference between the maximum and minimum density) for a 14 mm punch displacement (56% compression from initial fill height).

Observation from figure 13 reveals that density variation in the part increases with an increased friction value.

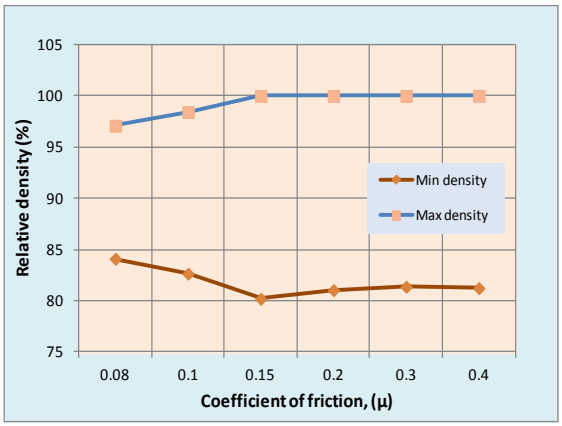

Fig. 13 Relative density Vs coefficient of friction

The density variation along the contact interaction (between the powder and the die wall) for various 'μ' is plotted in figure 14. The maximum density obtained for all the cases is at uppermost and lowermost nodes. Whereas the minimum density obtained is at central node.

The slope of the graph is constantly varying when 'μ' ranges from 0.15 to 0.2 and also attain 100% relative density. Whereas for higher value of 'μ'; larger band of low density distribution near the central region makes part ineffective for the central loading application.

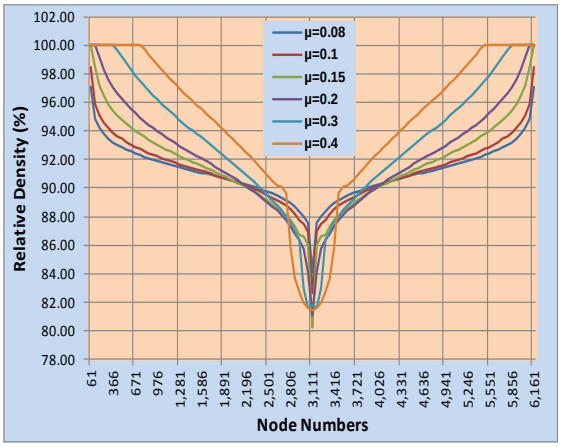

Fig. 14 Density variations along the die wall interaction

A better density distribution and comparatively denser parts can be produced by maintaining friction coefficient 0.15<μ<0.2.

6.3 Results: Effect of Height to Diameter (H/D) Ratio

In order to get different H/D ratios; height of the powder fill was varied by keeping diameter (30mm) of the specimen constant.

The variation in relative density versus H/D is plotted in the figure 15. From figure 15, it can be observed that the maximum relative density increases whereas minimum density decreases when initial fill height increases.

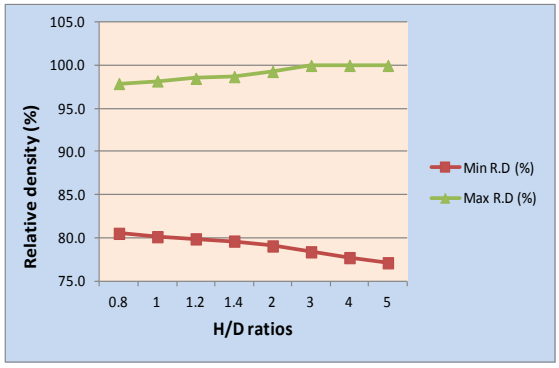

Fig. 15 Relative density Vs H/D ratios

The relative density corresponding to various H/D are tabulated under table 1.

H/D Ratio	0.8	1	1.2	1.4	2	3	4	5
Fill Height (mm)	24	30	36	42	60	90	120	150
Min R.D (%)	80.5	80.1	79.9	79.6	79.1	78.4	77.7	77.1
Max R.D (%)	97.9	98.2	98.5	98.7	99.3	100	100	100

Table 1. Relative density for various H/D ratios

From figure 15, it can be observed that as punch travel distance is more for greater H/D compact; it results 100% density at upper and lower punches location whereas minimum density in the compact keeps reducing due to large pressure drop toward the center of the compact. Figure 16 illustrates the plot between axial stresses versus different initial powder fill height (H/D ratio).

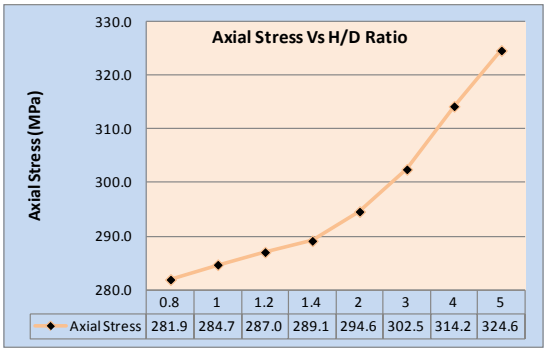

Fig. 16 Axial stress Vs H/D ratios

The observation from figure 16 reveals that, more axial stresses are induced in the compact when higher H/D ratio is taken. Hence it is recommended to limit the H/D ratio. H/D ratio recommended for obtaining higher and uniform relative density for 56% compaction is 2-3. Higher H/D will result in large variation in relative density distribution whereas lower H/D result in less than 100% density in any portion of the compact.

7. CONCLUSIONS

Numerical modeling of the powder metallurgy die compaction process provides a cost- effective and efficient method to establish procedure to attain desired compact properties. Constitutive material models developed to study soil behavior under consolidation loads can be used to define the behavior of the material under compaction loads. The Cam-Clay model can describe the loose powder response and the particle deformation. Water atomized 601AB aluminium powder was selected for this work due to their industrial application. A numerical model using the Cam-Clay model has been formulated in the commercially available finite element software ABAQUS to model the die compaction process. While the model is formulated for a simple axi-symmetric geometry, it can be extended to more complex geometries.

From the study we found that the maximum height compression is ~55-56% of the original height (in this case 50*0.56=28 mm) for 601AB alloy. A better density distribution and comparatively denser parts can be produced by maintaining friction coefficient $0.15<\mu<0.2$. H/D ratio recommended for obtaining higher and uniform relative density for 56% compaction is 2-3. Higher H/D will result in large variation in relative density distribution whereas lower H/D result in less than 100% density in any portion of the compact.

8. REFERENCES

[1] ASM Handbook., Powder Metal Technologies and applications, Volume 7 ASM international

[2] http://www.substech.com retrieved on 19 February 2012

[3] G. S. Wagle, *Die compaction simulation*-simplifying the application of a complex constitutive model using numerical and physical experiments, Pennsylvania state university, 2006.

[4] F. Sánchez, A. Bolarín, J. Coreño, A. Martínez and J.A. Bas Effect of the Compaction Process sequence on the Axial Density Distribution of Green Compacts. Powder Metallurgy., Institute of Materials, IoM Communications, Vol. 44, no. 4, pp. 1-5, 2001.

[5] ABAQUS, *Users Manual*, Version 6.10-1, from SIMULIA

[6] K. Vara Prasada Rao . *Manufacturing Science and Technology* - Manufacturing Processes and Machine Tools, New Age International pp. 141-145, 2002

[7] Cong Lu, Determination of Cap Model Parameters using Numerical Optimization Method for Powder Compaction, Marquette University, 2009

[8] L-H. Moon, K.H. Kim Relationship between compacting pressure, green density and green strength of copper powder compacts, Powder Metallurgy, 27 (2) (1984) 80-84.

[9] I. Aydin, B. J. Briscoe, N. Ozkan, .Modeling of Powder Compaction: A Review., *MRS Bulletin*, December 1997, pp. 45 . 51.